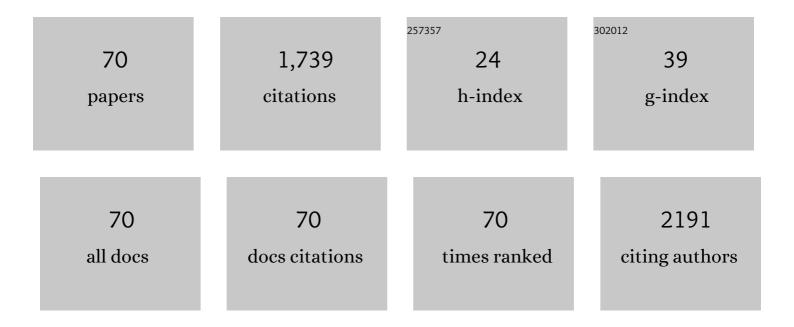
List of Publications by Year in descending order

Source: https://exaly.com/author-pdf/2614887/publications.pdf Version: 2024-02-01



#	Article	IF	CITATIONS
1	Tuning of the Size of Dy ₂ O ₃ Nanoparticles for Optimal Performance as an MRI Contrast Agent. Journal of the American Chemical Society, 2008, 130, 5335-5340.	6.6	117
2	MRI contrast agents based on dysprosium or holmium. Progress in Nuclear Magnetic Resonance Spectroscopy, 2011, 59, 64-82.	3.9	116
3	Fabrication of high quality anodic aluminum oxide (AAO) on low purity aluminum—A comparative study with the AAO produced on high purity aluminum. Electrochimica Acta, 2013, 105, 424-432.	2.6	109
4	NMR Transversal Relaxivity of Suspensions of Lanthanide Oxide Nanoparticles. Journal of Physical Chemistry C, 2007, 111, 10240-10246.	1.5	67
5	Review Article: Recommended reading list of early publications on atomic layer deposition—Outcome of the "Virtual Project on the History of ALDâ€. Journal of Vacuum Science and Technology A: Vacuum, Surfaces and Films, 2017, 35, .	0.9	65
6	Fast Fourier transform based arrangement analysis of poorly organized alumina nanopores formed via self-organized anodization in chromic acid. Materials Letters, 2014, 117, 69-73.	1.3	62
7	Fabrication of anodic aluminum oxide with incorporated chromate ions. Applied Surface Science, 2012, 259, 324-330.	3.1	58
8	The impact of viscosity of the electrolyte on the formation of nanoporous anodic aluminum oxide. Electrochimica Acta, 2014, 133, 57-64.	2.6	50
9	Mg2NiH4 synthesis and decomposition reactions. International Journal of Hydrogen Energy, 2013, 38, 4003-4010.	3.8	44
10	Ethanol influence on arrangement and geometrical parameters of aluminum concaves prepared in a modified hard anodization for fabrication of highly ordered nanoporous alumina. Journal of Electroanalytical Chemistry, 2015, 750, 79-88.	1.9	44
11	Monolithic porous graphitic carbons obtained through catalytic graphitization of carbon xerogels. Journal of Physics and Chemistry of Solids, 2013, 74, 101-109.	1.9	43
12	The influence of electrolyte composition on the growth of nanoporous anodic alumina. Electrochimica Acta, 2016, 211, 453-460.	2.6	43
13	UV plasmonic-based sensing properties of aluminum nanoconcave arrays. Current Applied Physics, 2014, 14, 1514-1520.	1.1	41
14	A comparative study of electrochemical barrier layer thinning for anodic aluminum oxide grown on technical purity aluminum. Journal of Electroanalytical Chemistry, 2015, 741, 80-86.	1.9	37
15	Hierarchical, nanoporous graphenic carbon materials through an instant, self-sustaining magnesiothermic reduction. Carbon, 2016, 96, 937-946.	5.4	37
16	Ultra-small nanopores obtained by self-organized anodization of aluminum in oxalic acid at low voltages. Materials Letters, 2013, 111, 20-23.	1.3	36
17	Synthesis and decomposition mechanisms of ternary Mg2CoH5 studied using in situ synchrotron X-ray diffraction. International Journal of Hydrogen Energy, 2011, 36, 10760-10770.	3.8	34
18	Controlling of water wettability by structural and chemical modification of porous anodic alumina (PAA): Towards super-hydrophobic surfaces. Surface and Coatings Technology, 2015, 276, 464-470.	2.2	33

#	Article	IF	CITATIONS
19	Effect of ethylene glycol on morphology of anodic alumina prepared in hard anodization. Journal of Electroanalytical Chemistry, 2016, 762, 20-28.	1.9	33
20	Morphology and Transport Rates of Mixed IV–VI Compounds in Microâ€Gravity. Journal of the Electrochemical Society, 1977, 124, 1095-1102.	1.3	32
21	A simple method of synthesis and surface purification of titanium carbide powder. International Journal of Refractory Metals and Hard Materials, 2013, 38, 87-91.	1.7	32
22	Heterogeneous iron-containing carbon gels as catalysts for oxygen electroreduction: Multifunctional role of sulfur in the formation of efficient systems. Carbon, 2017, 116, 655-669.	5.4	31
23	1H Relaxivity of Water in Aqueous Suspensions of Gd3+-Loaded NaY Nanozeolites and AlTUD-1 Mesoporous Material:Â the Influence of Si/Al Ratio and Pore Size. Inorganic Chemistry, 2007, 46, 6190-6196.	1.9	30
24	Anodization of cold deformed technical purity aluminum (AA1050) in oxalic acid. Surface and Coatings Technology, 2014, 258, 268-274.	2.2	24
25	Catalytic stability and surface analysis of microcrystalline Ni3Al thin foils in methanol decomposition. Applied Surface Science, 2014, 293, 169-176.	3.1	23
26	Plasmonic enhancement of blue emission from ZnO nanorods grown on the anodic aluminum oxide (AAO) template. Applied Physics A: Materials Science and Processing, 2013, 111, 265-271.	1.1	22
27	Incorporation of copper chelate ions into anodic alumina walls. Materials Letters, 2013, 106, 242-245.	1.3	22
28	Nanoporous alumina formed by self-organized two-step anodization of Ni3Al intermetallic alloy in citric acid. Applied Surface Science, 2013, 264, 605-610.	3.1	21
29	Heterogeneous Carbon Gels: N-Doped Carbon Xerogels from Resorcinol and N-Containing Heterocyclic Aldehydes. Langmuir, 2014, 30, 14276-14285.	1.6	21
30	Approaches to enhance UV light emission in ZnO nanomaterials. Current Applied Physics, 2019, 19, 867-883.	1.1	20
31	Study on the correlation between criterion number derived from Rayleigh–Bénard convective cells and arrangement of nanoporous anodic aluminum oxide. Materials Letters, 2014, 125, 124-127.	1.3	19
32	Copolycondensation of heterocyclic aldehydes: A general approach to sulfur and nitrogen dually-doped carbon gels. Microporous and Mesoporous Materials, 2016, 225, 198-209.	2.2	19
33	In-situ electrochemical doping of nanoporous anodic aluminum oxide with indigo carmine organic dye. Thin Solid Films, 2016, 598, 60-64.	0.8	18
34	A comparative study on the hydrogen absorption of thin films at room temperature deposited on non-porous glass substrate and nano-porous anodic aluminum oxide (AAO) template. International Journal of Hydrogen Energy, 2011, 36, 11777-11784.	3.8	17
35	Fabrication and geometric characterization of highly-ordered hexagonally arranged arrays of nanoporous anodic alumina. Polish Journal of Chemical Technology, 2014, 16, 63-69.	0.3	17
36	Plasmonic enhancement of UV emission from ZnO thin films induced by Al nano-concave arrays. Applied Surface Science, 2016, 384, 18-26.	3.1	16

#	Article	IF	CITATIONS
37	Spectroscopy and Photophysics of Monoazaphenanthrenes I. Absorption and Fluorescence Spectra of Phenanthridine and 7,8-Benzoquinoline. Acta Physica Polonica A, 2003, 104, 425-439.	0.2	16
38	Tailoring UV emission from a regular array of ZnO nanotubes by the geometrical parameters of the array and Al 2 O 3 coating. Ceramics International, 2017, 43, 5693-5701.	2.3	15
39	Carbide-derived carbon obtained via bromination of titanium carbide: Comparative analysis with chlorination and hydrogen storage studies. Microporous and Mesoporous Materials, 2019, 273, 26-34.	2.2	15
40	NMR Transversal relaxivity of aqueous suspensions of particles of Ln3+-based zeolite type materials. Dalton Transactions, 2008, , 2241.	1.6	14
41	Morphological, structural and optical characterization of SnO2 nanotube arrays fabricated using anodic alumina (AAO) template-assisted atomic layer deposition. Materials Characterization, 2018, 136, 52-59.	1.9	13
42	Morphological and chemical characterization of highly ordered conical-pore anodic alumina prepared by multistep citric acid anodizing and chemical etching process. Journal of Porous Materials, 2018, 25, 45-53.	1.3	13
43	Tailoring of UV/violet plasmonic properties in Ag, and Cu coated Al concaves arrays. Applied Surface Science, 2014, 314, 807-814.	3.1	12
44	Influence of Anodization Temperature on Geometrical and Optical Properties of Porous Anodic Alumina(PAA)-Based Photonic Structures. Materials, 2020, 13, 3185.	1.3	12
45	Fabrication and characterization of oxide nano-needles formed by copper passivation in sodium hydroxide solution. Thin Solid Films, 2019, 671, 111-119.	0.8	11
46	On-Aluminum and Barrier Anodic Oxide: Meeting the Challenges of Chemical Dissolution Rate in Various Acids and Solutions. Coatings, 2020, 10, 875.	1.2	11
47	Optical Properties of Porous Alumina Assisted Niobia Nanostructured Films–Designing 2-D Photonic Crystals Based on Hexagonally Arranged Nanocolumns. Micromachines, 2021, 12, 589.	1.4	11
48	H2 absorption at ambient conditions by anodized aluminum oxide (AAO) pattern-transferred Pd nanotubes occluded by Mg nanoparticles. Materials Chemistry and Physics, 2012, 133, 376-382.	2.0	10
49	Structural and Optical Characterization of ZnS Ultrathin Films Prepared by Low-Temperature ALD from Diethylzinc and 1.5-Pentanedithiol after Various Annealing Treatments. Materials, 2019, 12, 3212.	1.3	10
50	Peculiar Porous Aluminum Oxide Films Produced via Electrochemical Anodizing in Malonic Acid Solution with Arsenazo-I Additive. Materials, 2021, 14, 5118.	1.3	10
51	The influence of pre-anodization voltage on pore arrangement in anodic alumina produced by hard anodization. Materials Letters, 2016, 183, 5-8.	1.3	9
52	Manufacturing of highly ordered porous anodic alumina with conical pore shape and tunable interpore distance in the range of 550 nm to 650 nm. Materials Science-Poland, 2017, 35, 511-518.	0.4	9
53	Origin of microporosity in chalcogen-doped carbon materials: The case of selenium-doped carbogels. Microporous and Mesoporous Materials, 2018, 272, 260-264.	2.2	9
54	Infrared Absorption Study of Zn–S Hybrid and ZnS Ultrathin Films Deposited on Porous AAO Ceramic Support. Coatings, 2020, 10, 459.	1.2	9

#	Article	IF	CITATIONS
55	Oxidative and adsorptive removal of chlorophenols over Fe-, N- and S-multi-doped carbon xerogels. Journal of Environmental Chemical Engineering, 2021, 9, 105568.	3.3	9
56	Multi-band emission in a wide wavelength range from tin oxide/Au nanocomposites grown on porous anodic alumina substrate (AAO). Applied Surface Science, 2013, 287, 143-149.	3.1	8
5 7	Towards Self-Organized Anodization of Aluminum in Malic Acid Solutions—New Aspects of Anodization in the Organic Acid. Materials, 2020, 13, 3899.	1.3	8
58	Fabrication of Porous Anodic Alumina (PAA) by High-Temperature Pulse-Anodization: Tuning the Optical Characteristics of PAA-Based DBR in the NIR-MIR Region. Materials, 2020, 13, 5622.	1.3	8
59	Advanced Image Analysis of the Surface Pattern Emerging in Ni3Al Intermetallic Alloys on Anodization. Frontiers in Materials, 2016, 3, .	1.2	7
60	Revisiting semicontinuous silver films as surface-enhanced Raman spectroscopy substrates. Beilstein Journal of Nanotechnology, 2019, 10, 1048-1055.	1.5	7
61	Peculiarities of Aluminum Anodization in AHAs-Based Electrolytes: Case Study of the Anodization in Glycolic Acid Solution. Materials, 2021, 14, 5362.	1.3	6
62	Anodic alumina growth on Al substrates after multi-variant mechanical and heat treatment. Surface and Coatings Technology, 2019, 357, 802-810.	2.2	5
63	Spectroscopy and Photophysics of Monoazaphenanthrenes III. Luminescence of Phenanthridine and 7,8-benzoquinoline in Crystalline State. Acta Physica Polonica A, 2004, 106, 77-94.	0.2	5
64	Effect of Various Electrolyte Modifiers on Anodic Alumina (AAO) Growth and Morphology. Current Nanoscience, 2018, 15, 76-83.	0.7	5
65	Charge Density-Versus Time-Controlled Pulse Anodization in the Production of PAA-Based DBRs for MIR Spectral Region. Energies, 2021, 14, 5149.	1.6	4
66	Systematic Study on Morphology of Anodic Alumina Produced by Hard Anodization in the Electrolytes Modified with Ethylene Glycol. Journal of Nano Research, 2017, 46, 165-178.	0.8	2
67	Optimization of UV luminescence from ZnO thin film: A combined effect of Al concave arrays and Al2O3 coating. Materials Letters, 2018, 229, 185-188.	1.3	2
68	Recent Advances in Metal, Ceramic, and Metal–Ceramic Composite Films/Coatings. Coatings, 2022, 12, 571.	1.2	1
69	Improved anti-reflective properties of amorphous silicon films deposited on Al nanoconcave arrays. Materials Letters, 2014, 135, 199-201.	1.3	0
70	Moth-Eye Mimicking By Electrochemical Oxidation Of Aluminum. , 2018, , .		0